

## STRUCTURAL SAFETY OF HIGH ARCH DAMS WITH VARIABLE WATER LEVELS BASED ON SEISMIC PERFORMANCE EVALUATION\*

M. A. HARIRI-ARDEBILI<sup>1\*\*</sup>, H. MIRZABOZORG<sup>2</sup> AND M. R. KIANOUSH<sup>3</sup>

<sup>1</sup>Dept. of Civil Environmental and Architectural Engineering, University of Colorado, Boulder, USA  
Email: mohammad.haririardabili@colorado.edu

<sup>2</sup>Dept. of Civil Engineering, K. N. Toosi University of Technology, Tehran, I. R. of Iran

<sup>3</sup>Dept. of Civil Engineering, Ryerson University, Toronto, Canada

**Abstract**– Seismic performance evaluation of arch dams under different environmental conditions is vital for the structural safety of the existing dams. In the present paper, effects of the reservoir water in four different levels are investigated on the seismic performance of an arch dam. Dynamic equilibrium equations of the dam-reservoir-massless foundation coupled system are solved by Newmark's time integration algorithm. Several three-component ground motions, obtained from deterministic hazard analysis of the dam site, are used for excitation of the finite element model. Seismic performance evaluation is utilized considering parameters such as crest displacement, demand capacity ratio, cumulative inelastic duration and extension of the overstressed areas on upstream and downstream faces obtained from linear elastic analyses. It is found that dewatering the reservoir leads to extension of the overstressed areas on both upstream and downstream faces and increases structural operating risk. In such a case, detailed nonlinear analyses, including joint and material nonlinearities, are required for more realistic results on crack propagation.

**Keywords**– Seismic performance evaluation, variable water level, arch dam, demand capacity ratio, cumulative inelastic duration

### 1. INTRODUCTION

Arch dams are very complicated infrastructures and their performance can be treated by various natural phenomena like floods, rockslides, earthquakes, deterioration of concrete material or even artificial (abnormal) events such as explosion, attack, and mismanagement of the dam hydropower system. However, earthquake ground motion is the most critical parameter in design and/or evaluation of the structural behavior of concrete dams, especially in high seismicity areas. Seismic behavior of dams depends on various factors like age, seismicity of the dam site, probable existing cracks within the dam body and/or foundation rock, history of the experienced strong ground motions and finally, reservoir water level. Reservoir water level and interaction between the dam and water is one of the key factors affecting seismic performance of the arch dams during earthquake. Reservoir water level usually varies based on the operational regime, the annual weathering conditions and sometimes reservoir level may be decreased to visit upstream face or to repair probable damages or even because of drought [1].

Importance of the hydrodynamic pressure on the structural behavior of dam has been studied by Fok and Chopra [2, 3], Fahjan *et al.* [4], Calayir *et al.* [5], Proulx *et al.* [6], Lin *et al.* [7], and Miquel and Bouaanani [8]. Akkose *et al.* [9] studied reservoir water level effects on nonlinear dynamic response of arch dams. Concrete was idealized as elasto-plastic using Drucker-Prager model and the reservoir was modeled by Lagrangian finite elements. Hacıefendioğlu *et al.* [10] studied seismic behavior of concrete

---

\*Received by the editors January 16, 2013; Accepted December 17, 2013.

\*\*Corresponding author

gravity dams when the reservoir is covered by ice. Mirzabozorg *et al.* [11] considered the effects of spatially varying ground motion on nonlinear response of an arch dam using Eulerian fluid elements. Hariri-Ardebili and Mirzabozorg [12] studied seismic response of a double symmetric arch dam under near-fault and far-field ground motions. They used Lagrangian-Eulerian approach for modeling the dam-water interaction. Also, Hariri-Ardebili and Mirzabozorg [13] investigated the effects of reservoir water fluctuations in crack propagation of an asymmetry high arch dam. They found that water level has significant structural effect and can increase the percentage of the cracked area in both upstream (US) and downstream (DS) faces of the dam body.

On the other hand, seismic performance and safety evaluation of hydraulic structures were studied by Ghanaat [14, 15], Yamaguchi *et al.* [16], Bayraktar *et al.* [17], and Hariri-Ardebili and Mirzabozorg [18 and 19]. Ghanaat [15] proposed a methodology for damage estimation in concrete dams which can be found in the USACE guideline [20]. In this guideline, a systematic method based on linear time-history results in terms of local and global performance indices was suggested. Empirical performance criteria are defined in terms of these indices and they form a basis for qualitative estimation of damage.

In the present paper, the pre-defined criteria for seismic performance evaluation of concrete dams are applied on a high arch dam considering the effect of various reservoir water levels. The structural safety of the arch dam is evaluated and the applicability and possible shortcomings of the introduced performance evaluation methodology is investigated.

## 2. PRINCIPLES OF SEISMIC PERFORMANCE EVALUATION

### a) Methodology

Usually, safety and serviceability of large mass concrete structures is controlled by tensile behavior of material. Actual response of massive concrete structures to earthquake ground motions is very complex. Loading histories and rapid seismic strain rates have an important role in structural performance [20]. The typical tensile stress-strain curve of mass concrete can be divided into three parts, i.e. serviceability, damage control, and collapse prevention performance. A linear elastic analysis combined with a predefined performance evaluation criteria can be used to assess dam response in the damage control range. Dam response beyond the damage control range is governed by complete loss of the strength, sliding, and nonlinear response behavior of discrete blocks bounded by opened joints and cracked sections and must be evaluated using nonlinear time-history analysis [20]. Fig.1 describes general flowchart for seismic performance evaluation of concrete arch dams.

### b) Indices

Seismic performance of concrete arch dams is evaluated in accordance with displacements, stresses, demand capacity ratio (DCR), cumulative inelastic duration (CID) and spatial extension of overstressed areas ( $A_{\text{overstressed}}$ ) on upstream and downstream faces of the dam body.

For arch dams where high stresses usually oriented in the arch and cantilever directions, DCR refers to the ratio of calculated arch or cantilever stress to tensile strength of mass concrete, but it can also be developed for principal stresses [15]. Tensile strength used in calculating DCR is obtained from uniaxial splitting tension tests or from Raphael's proposed diagram. The maximum permitted DCR for linear analysis of dams is 2.0. This corresponds to a stress demand twice the tensile strength of mass concrete. Different definitions of DCR can be summarized as:

$$DCR_a = \frac{\text{arch stress demand}}{\text{tensile strength}} = \frac{S_a}{f'_t} \quad (1)$$

$$DCR_c = \frac{\text{cantilever stress demand}}{\text{tensile strength}} = \frac{S_c}{f'_t} \quad (2)$$

$$DCR_p = \frac{\text{first principal stress demand}}{\text{tensile strength}} = \frac{S_1}{f'_t} \quad (3)$$

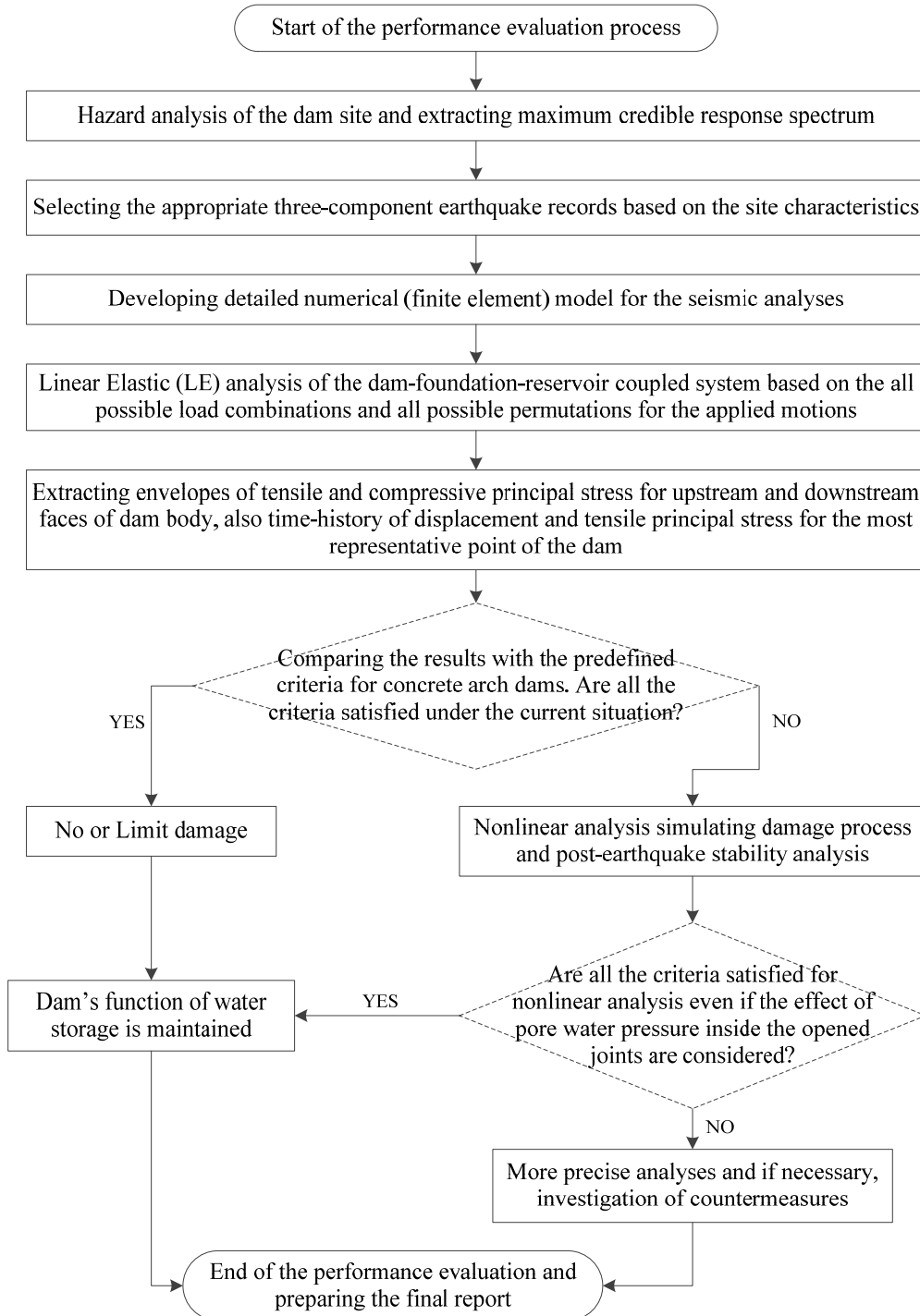


Fig. 1. General flowchart for seismic performance and safety evaluation of concrete arch dams

Cumulative inelastic or overstress duration, which is a measure of energy, accounts for magnitudes as well as duration of stresses exceeding it. It refers to the total time duration of stress exceeding from a stress level associated with a certain DCR [15]. For assessing the level of damage, CID is utilized in

conjunction with DCR. The performance threshold curve (PTC) for arch dams and the location of three performance levels are shown in Fig. 2 [15, 20]. Also, this figure can be used for the interpretation of the extracted results as recommended by USACE [20].

In addition to foregoing performance criteria, the damaged areas are required to be bounded in small regions, so that the evaluation on the basis of linear elastic analysis is still valid. Based on the USACE guideline [20], if the overstressed area is limited to 20% of total areas on US or DS faces, LE analysis is valid for seismic performance evaluation of concrete arch dams.

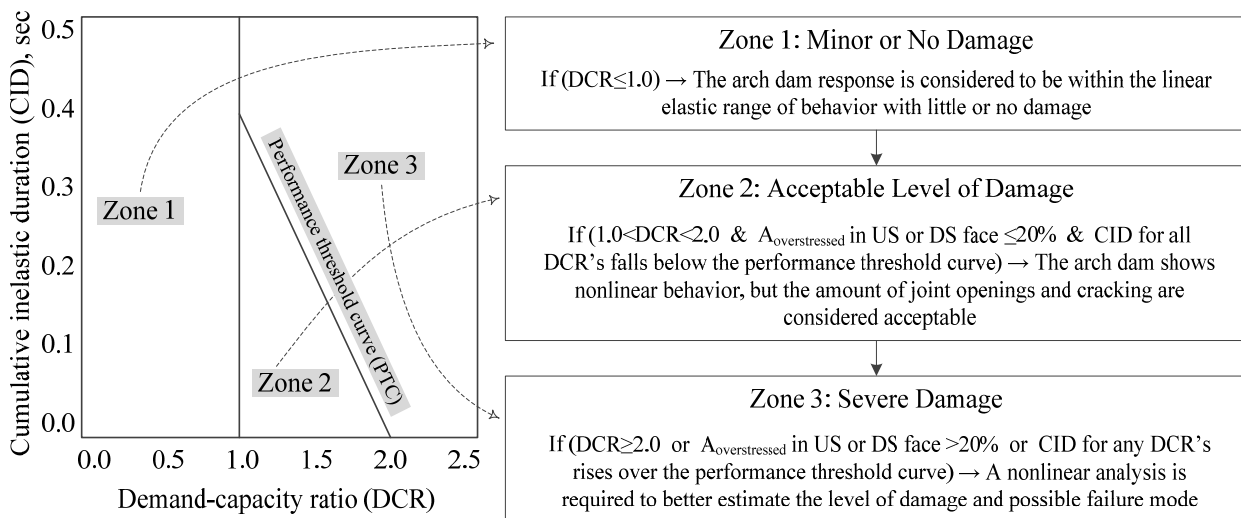


Fig. 2. Three performance zones and interpretation of the results for arch dams

### 3. EARTHQUAKE GROUND MOTIONS

Earthquake ground motions are defined based on source characteristics, source-to-site transmission path properties, and site conditions. Many factors like source depth, size of rupture area, style of faulting, shear-wave velocity, damping characteristics of crustal rock, rock properties, local soil conditions at the site and topography of the site must be considered for extracting site-specific ground motions [20, 21].

Generally, there are two approaches for determination of the site-specific response spectra, i.e. deterministic and probabilistic approaches. In the present study, results obtained from deterministic method, which is usually used for defining Maximum Credible Earthquake (MCE) are utilized. In this approach, typically one or more earthquakes are selected by magnitude and location with respect to the site. Various attenuation models have been suggested for this approach. For the considered dam site, three attenuation models were used; i.e., Ambraseys and Douglas [22], Campbell and Bozorgnia [23] and Boore *et al.* [24]. Peak ground horizontal acceleration (PHGA) was extracted as 0.412g, 0.538g and 0.483g based on Ambraseys and Douglas, Campbell and Bozorgnia and Boore *et al.*'s methods respectively. Peak ground vertical acceleration (PGVA) was extracted as 0.263g and 0.437g based on Ambraseys and Douglas, and Campbell and Bozorgnia's methods respectively. Finally, the mean values for PHGA and PVGA were calculated to be 0.478g and 0.350g respectively.

After hazard analysis of the dam site, design spectrums for horizontal and vertical components were extracted considering  $\xi=5\%$  as shown in Fig. 3. In the current study, Tabas, Manjil and Duzce earthquake records which are compatible with the dam site characteristics were selected and scaled based on acceleration response spectrum. Duration of the selected part of the ground motions was limited to 75% of the total Arias Intensity of the original motion, in order to save the computational efforts.

In 3D time-history analysis of arch dams, static loads and earthquake ground motion components should be combined in accordance with all possible permutations. Generally, a complete permutation of all three components with positive and negative signs is required to obtain the most critical directions that would cause the largest structural response [25]. Based on analyses conducted by the authors the most critical directions were detected for the present study.

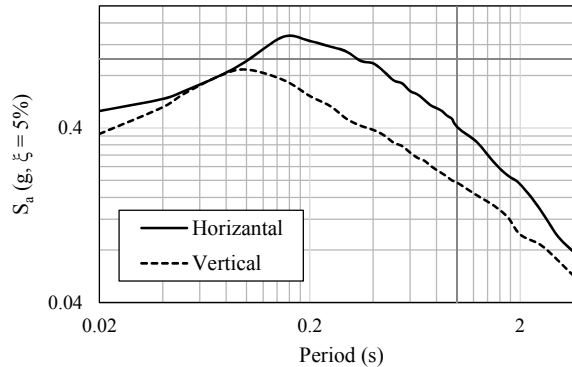


Fig. 3. Design response spectrum of the considered site in maximum credible level

#### 4. NUMERICAL EXAMPLE

A high double curvature arch dam was selected as numerical example. Total height of the dam is 203m, while the height above the concrete plug (the simulated dam) is 194m. Also, the height of the main body (without concrete saddle) is 186m. Thickness of the dam at the crest is 4.5m and its maximum thickness at the base is 21m. Generally, this dam is categorized as asymmetry slender dam and so its behavior should be studied precisely [26].

The provided finite element model shown in Fig.4a includes 792 solid elements for simulating the dam body. In this model, mostly hexagonal elements were used, while prism elements were utilized at portions of the model where geometry was not regular. In addition, 3770 hexagonal elements were used for modeling massless foundation rock. Far-end boundary of the foundation was located at a distance from the dam body which is about twice the dam height in all directions. The reservoir was modeled using hexagonal and prism fluid elements. Utilized fluid elements have three translational degree-of-freedom (DOFs) and one pressure DOF at each node. It should be noted that translational DOFs are active only at nodes that are on the interface with solid elements. The coupled equations of the dam-foundation-reservoir take the form:

$$\begin{cases} [M]\{\ddot{U}\} + [C]\{\dot{U}\} + [K]\{U\} = \{f_1\} - [M]\{\ddot{U}_g\} + [Q]\{P\} = \{F_1\} + [Q]\{P\} \\ [G]\{\ddot{P}\} + [C']\{\dot{P}\} + [K']\{P\} = \{F\} - \rho[Q]^T (\{\ddot{U}\} + \{\ddot{U}_g\}) = \{F_2\} - \rho[Q]^T \{\ddot{U}\} \end{cases} \quad (4)$$

where  $[M]$ ,  $[C]$  and  $[K]$  are the mass, damping and stiffness matrices of the structure including the dam body and its foundation media and  $[G]$ ,  $[C']$  and  $[K']$  represent the mass, damping and stiffness equivalent matrices of the reservoir, respectively. The matrix  $[Q]$  is the coupling matrix;  $\{f_1\}$  is the vector including both the body and the hydrostatic force;  $\{P\}$  and  $\{U\}$  are the vectors of hydrodynamic pressures and displacements, respectively and  $\{\ddot{U}_g\}$  is the ground acceleration vector. The coupled equations are solved using the staggered method in which the direct integration scheme is used to determine the displacement and hydrodynamic pressure at time increment  $i+1$  [27].

Boundary conditions on the reservoir water and their mathematical equations are shown in Fig.4b where  $n$ ,  $a_n^{struc}$  and  $\alpha_0$  are outwardly normal direction to the dam body, the normal acceleration on the dam,

and the wave reflection coefficient at the foundation-reservoir interface respectively [27].  $C_0$  is the pressure wave velocity in the liquid and  $\rho_w$  is the mass density of the water. It assumes that there is no penetration at the dam-reservoir interface and so all the waves reflected completely from the dam face, however, partial absorption is considered at the reservoir-foundation interface. Impedance ratio is assumed to be unity at the far-end boundary of the reservoir in order to fully absorb the outgoing waves. Finally, zero pressure boundary condition is considered at the reservoir free surface and sloshing effects are neglected due to height of the dam [27].

Material properties for mass concrete and foundation rock obtained from instrumentation and site observation are summarized in Table 1 [26]. It should be mentioned that due to the inherent rate dependence of the mechanical and strength properties of mass concrete, the dynamic properties are different from the static properties [20]. Furthermore, reservoir water density is assumed  $1000\text{kg/m}^3$ , sound velocity is  $1440\text{m/s}$  in water, and wave reflection coefficient for reservoir around boundary is taken as 0.8, conservatively.

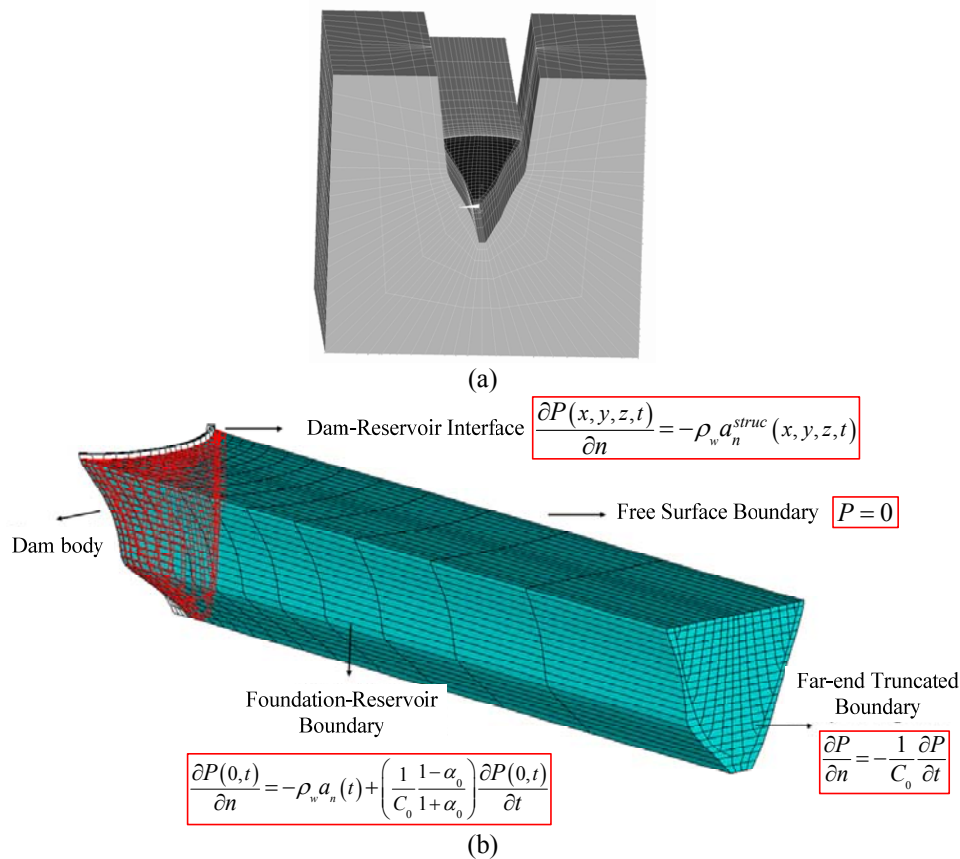


Fig. 4. (a) Finite element model of the dam-foundation-reservoir system; (b) Mathematical representation of the reservoir boundary conditions

Table. 1. Material properties of mass concrete and foundation rock

	Properties	Static values	Dynamic values
Mass concrete	Isotropic elasticity	40GPa	46GPa
	Poisson's ratio	0.2	0.14
	Mass density		2400 kg/m <sup>3</sup>
	Uniaxial compressive strength	35.0MPa	36.5MPa
	Uniaxial tensile strength	3.4MPa	5.1MPa
Foundation rock	Deformation modulus (saturated)		13GPa
	Deformation modulus (unsaturated)		15GPa
	Poisson's ratio		0.25

Applied loads on the system are dam body self weight, hydrostatic pressure in four various water levels and the earthquake loading. It should be noted that the thermal loads are not considered in the current study because the main objective of the paper is to consider the fluid-structure interaction on dam response. The Newmark- $\beta$  time integration method is utilized to solve the coupled problem of dam-reservoir-foundation model. The coupled system is excited at foundation boundaries using appropriate three-component earthquake records simultaneously. Structural damping is taken to be 10% of critical damping due to exciting the system in MCE level [20]. Water levels in the reservoir are considered as 56m, 101m, 155m and 188m that stand to level I, level II, level III and level IV. In the next section, the responses of the dam body subjected to Tabas ground motion is investigated in detail and the results of Manjil and Duzce ground motions are used to generalize the findings.

## 5. RESULTS AND DISCUSSION

Application of the USACE methodology does not depend on the reservoir capacity and the scale of the dam. Reservoir water level is an important factor in seismic performance evaluation of the concrete dams because it changes the condition of the applied loads on upstream face of dam. Based on this guideline, the reservoir at the normal water level (NWL), which is the highest water level in non-flood season, is recommended to be considered in seismic performance evaluation process. Some guidelines state that dams should be evaluated using other water levels in which dams are susceptible to effects of earthquakes. So in the present section, responses are studied based on existing criteria under various reservoir levels.

Time-histories of the crest displacement at the central cantilever as well as the static and maximum dynamic responses are shown in Fig.5. Considering that the positive direction of the axis is toward DS, it becomes evident from static results that in low levels of the reservoir, the dam body tends to move in US direction. Static displacement of the dam toward DS increases intensively by increasing reservoir level. As it becomes evident from dynamic analyses results, increase of the reservoir level from I to IV leads to increase in maximum displacement at the crest towards the DS direction and generally, movement of the crest in US direction decreases except in level I in comparison with level II.

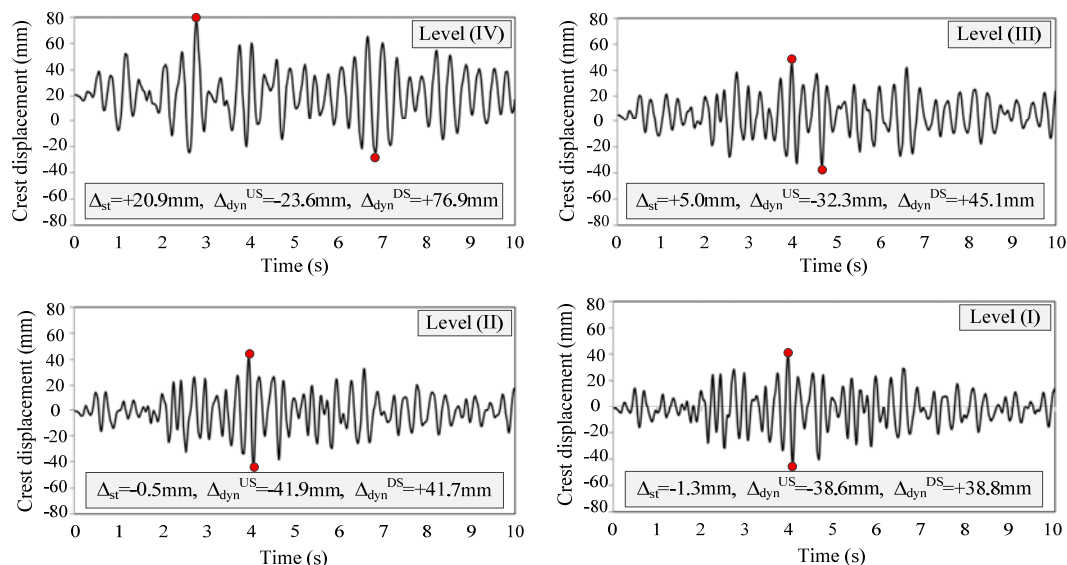


Fig. 5. Time-history of the crest displacement in stream direction

Non-concurrent envelope of the maximum and minimum principal stresses on US and DS faces of the dam body are shown in Figs. 6 and 7. As seen, dewatering reservoir increase maximum principal stresses within the dam body, especially in upper parts and in the vicinity of the crest. On the other hand,

impounding reservoir increases the area with high compressive stresses in the central upper part of US face and in upper parts in the vicinity of foundation on DS face.

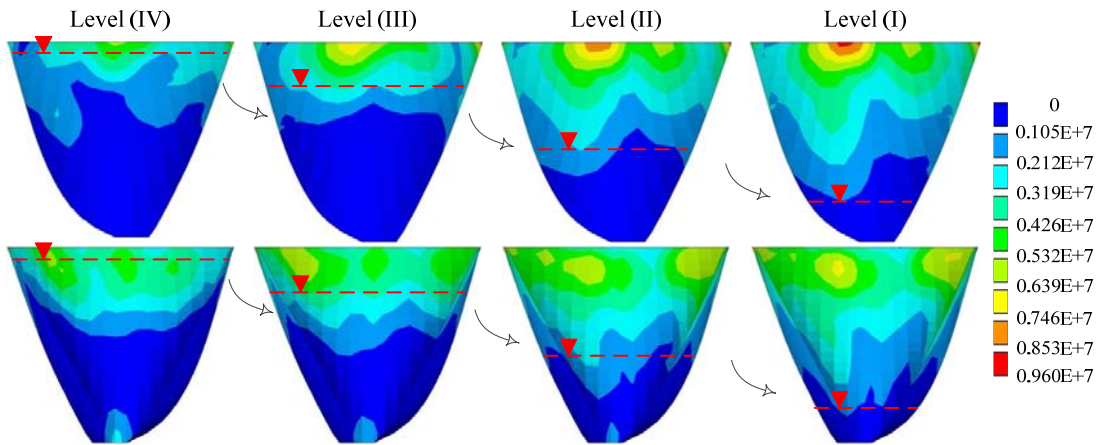


Fig. 6. Non-concurrent envelope of the maximum principal stresses on US and DS faces (Pa)

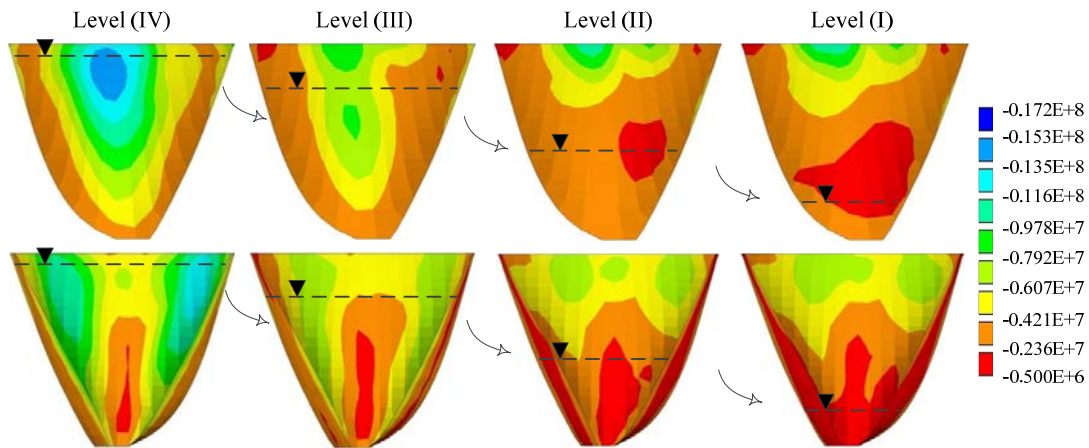


Fig. 7. Non-concurrent envelope of the minimum principal stresses on US and DS faces (Pa)

According to criteria introduced in previous sections, the most representative nodes on US and DS faces were selected in each model. Figure 8 shows the location of the selected nodes. Time-history of the maximum principal stress (tensile stress) and also, corresponding performance curves on CID-DCR diagram are displayed in Fig. 9 for various reservoir water levels. As expected from non-noncurrent stress envelopes, dewatering the reservoir increases the intensity of tensile stress during earthquake. The performance curves for both critical nodes on US and DS faces fall below PTC for level IV. In level III performance curve for the node on DS is always below PTC but for critical node on US the curve exceeds PTC at the beginning and the end of the curve. For reservoir level II, the performance curve on US node completely and the one on DS node partially exceed PTC and finally, for water in level I, the node located on US face extremely exceeds PTC but DS node partially exceeds predefined criteria.

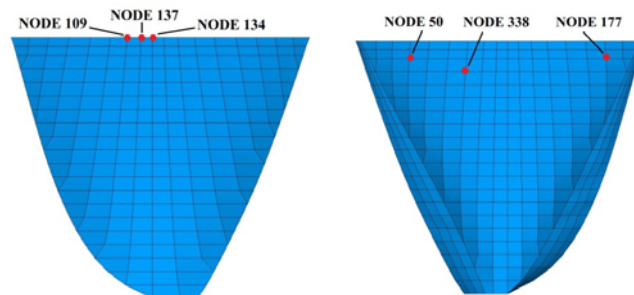


Fig. 8. Location of the critical nodes on US and DS faces



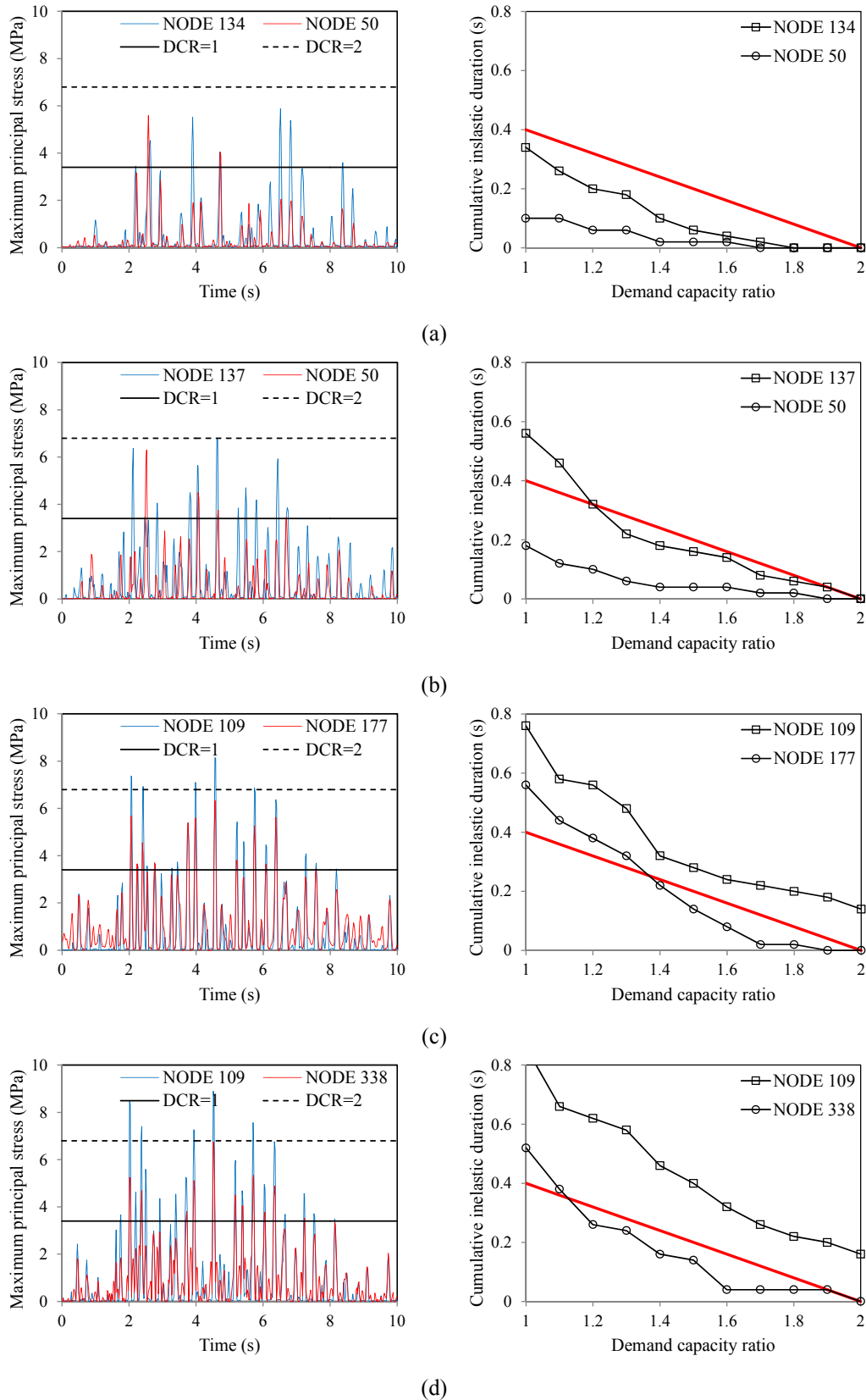


Fig. 9. Time-history of the maximum principal stress and the performance curves for the two most critical nodes on US and DS faces; (a) Level IV, (b) Level III, (c) Level II, (d) Level I

Figure 10 displays extension of the areas on US and DS faces in which CID exceeds threshold value for specific DCR in various water levels. It must be noted that only the upper quarter part of the dam body

is displayed in this figure. As is evident, extension of areas with exceeded CID decreases with reservoir impounding. Moreover, for levels I and II it is evident that the areas with high CID are extended in all DCRs. Based on USACE guidelines [20], the most representative or critical node is the node with highest tensile stress within the dam body. For the lowest water level (level I) these are nodes numbered as 109 on US and 338 on DS face. As shown in Fig. 9d, the curve for node 338 exceeds PTC only in DCR=1.0, but based on the first column of Fig. 10 the node located in the right upper part on DS (node number 177) exceeds PTC in DCR=1.0, 1.2 and 1.4. So it seems that selecting critical node only based on maximum tensile stress is not a completely perfect method for plotting performance curve, although it is enough for recognizing the adequacy of linear elastic analysis for seismic performance evaluation of the arch dams.

Figure 11 shows the extension of the overstressed areas on US and DS faces. As can be seen, dewatering the reservoir increases overstressed areas on both faces. Differences of the overstressed area between the levels I and II are negligible for both faces. Although the areas on US face for lower water levels are completely overlapped with those corresponding with higher levels, this is not true for DS face.

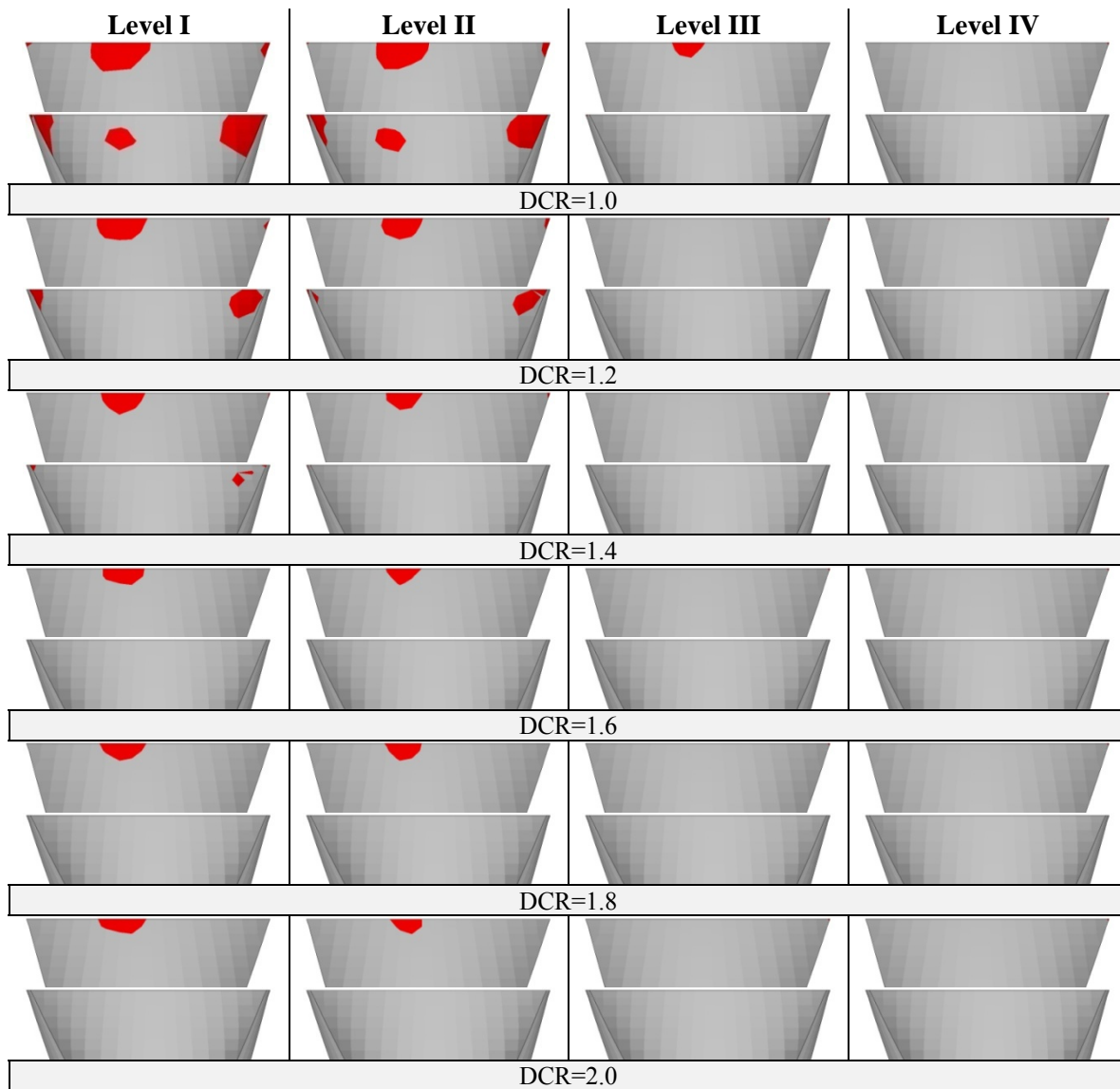


Fig. 10. Location of dam surfaces in which CID exceeds threshold value for specific DCRs

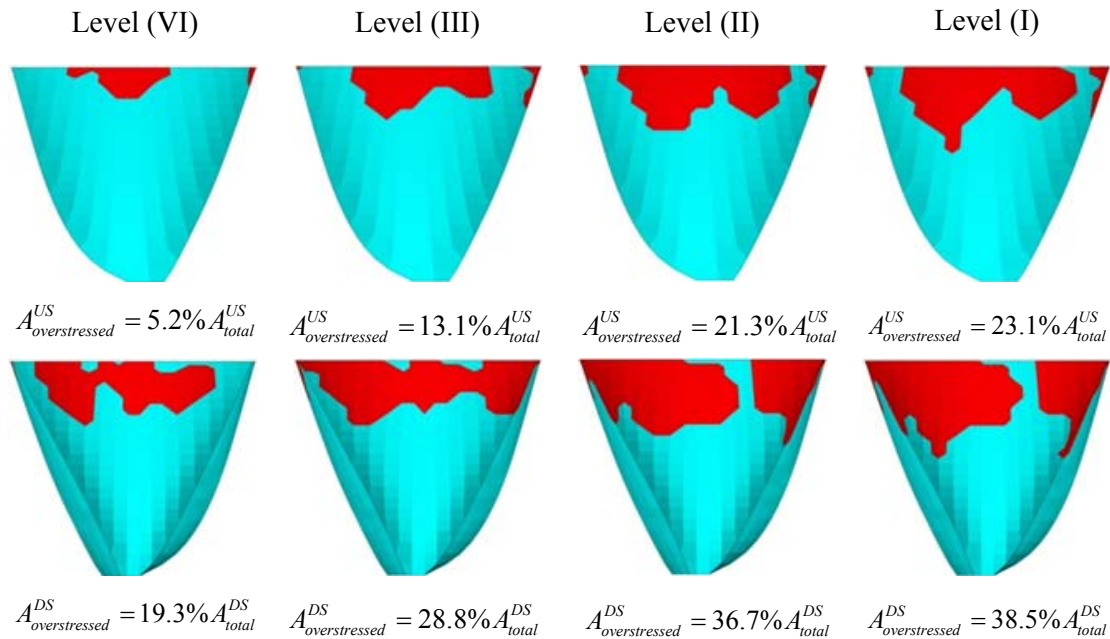


Fig. 11. Extension of the overstressed areas on US and DS faces

Based on the results presented in the previous section, discussion on performance evaluation of the considered dam in various water levels and adequacy of linear elastic analysis is given as follows:

- In level IV, DCR is always below 2.0; overstressed areas on both US and DS faces are limited to 20% and the performance curve always falls below PTC. Also, envelope of stresses within the dam body and the envelope of displacement along the central block are reasonable. Based on flowchart shown in Fig. 2, the dam is expected to behave in zone 2 and linear elastic analysis is adequate for this level of reservoir.
- In level III, DCR is always below 2.0; overstressed area reaches to 28.8% on DS face; performance curve exceeds partially from PTC and the envelope of stresses and displacement are reasonable. Based on flowchart (Fig. 2), the dam experiences some nonlinear behavior.
- In level II, DCR exceeds 2.0; overstressed area reaches to 36.7% on DS face; performance curve exceeds completely from PTC and the envelope of stresses and displacement are reasonable. Based on the flowchart in Fig. 2, the dam is expected to behave in zone 3 and nonlinear analysis must be conducted for capturing the possible severe damage or joint opening within the dam body.
- In level I, DCR exceeds 2.0 several times; overstressed area increases to 38.5% on DS face; performance curve extremely exceeds from PTC and the envelope of displacement is reasonable but high tensile stresses are observed in the upper part of the dam body. Based on pertinent flowchart, the dam experiences severe damage and it is highly recommended that nonlinear analysis is conducted considering opening/closing of joints and possible cracking at lift joints.

## 6. GENERALIZING RESEARCH FINDINGS

All the presented results in the previous sections are pertinent to exciting the coupled system using Tabas earthquake records. In the current section, the dam-reservoir-foundation system is excited using two other natural scaled earthquake records, i.e. Manjil and Duzce, and the results are compared with those obtained in previous sections.

Figure 12 represents non-concurrent displacement envelope for upstream nodes of the central cantilever based on three selected ground motions and also the average of them in each reservoir level. As it was shown, displacement envelope is critical when reservoir is in level IV (full reservoir) and dewatering the reservoir leads to decreasing displacements, especially in lower parts of the cantilever. Table 2 represents maximum absolute displacements experienced by the center, left and right quarter points of the dam crest under different ground motions. Based on this table, maximum displacement always occurs in level IV.

Figure 13 displays envelopes of the maximum first principal stress (S1) and minimum third principal stress (S3) along the height of the central cantilever. As is clear, generally dam experiences higher S1 when reservoir is in low levels. Also, resemblance of curves decreases for upper reservoir levels. In addition, increasing the water level increases the absolute value of the S3, especially for upper parts of the dam body.

Figure 14 shows the status of the most representative nodes on upstream and downstream faces of the dam body based on demand capacity ratio and also cumulative inelastic duration. As seen, for all ground motions the performance curves are below the predefined threshold in level IV. Performance curves of upstream nodes in level III partially exceed from PTC. For reservoir levels II and I, both upstream and downstream node's performance curves exceed from PTC but generally it is more critical for level I than level II.

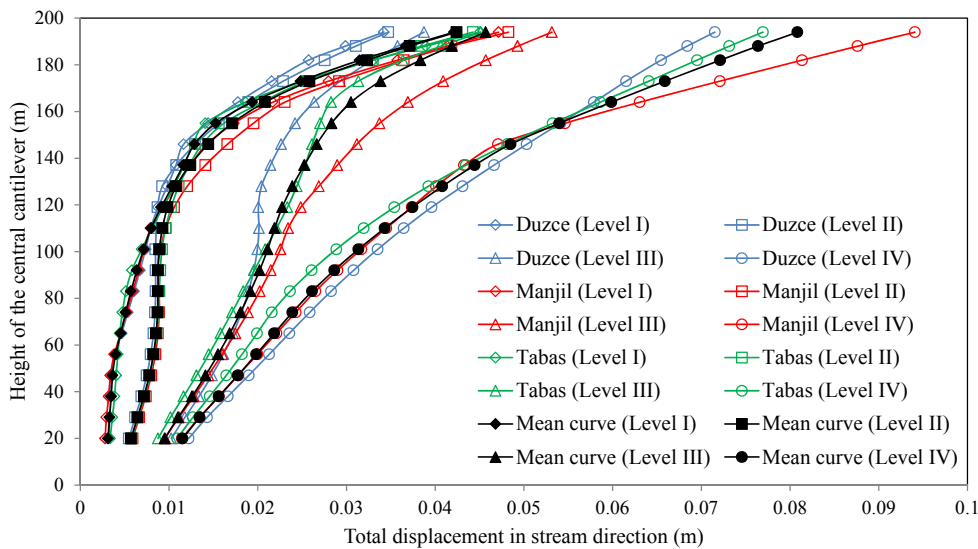


Fig. 12. Comparison of the non-concurrent displacement envelope of the central cantilever in stream direction for the three scaled ground motions

Table 2. Maximum absolute displacement of points at crest level subjected to different ground motions (mm)

Ground motion	Target point	Level I	Level II	Level III	Level IV
TABAS	Left quarter point	39.42	37.28	34.75	41.97
	Center point	45.06	44.25	45.15	76.93
	Right quarter point	26.47	25.34	21.08	34.08
MANJIL	Left quarter point	23.44	22.53	18.67	24.63
	Center point	47.14	48.26	53.16	94.07
	Right quarter point	34.44	31.79	27.56	38.16
DUZCE	Left quarter point	30.87	29.37	21.08	31.78
	Center point	34.20	34.72	38.73	71.51
	Right quarter point	43.24	42.60	34.95	50.03

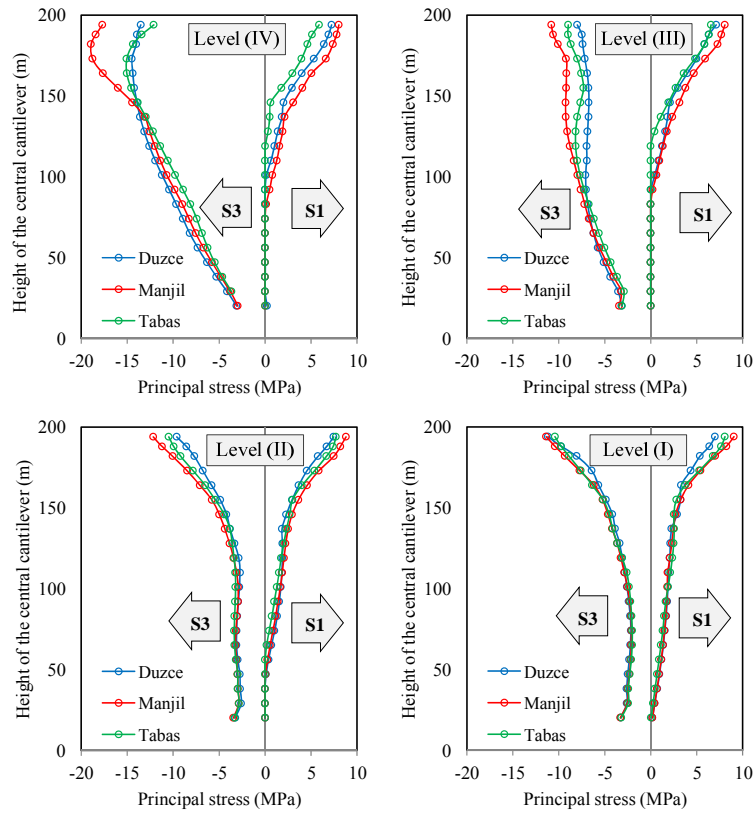


Fig. 13. Non-concurrent envelope of the maximum first principal stress and minimum third principal stress along the height of the central cantilever

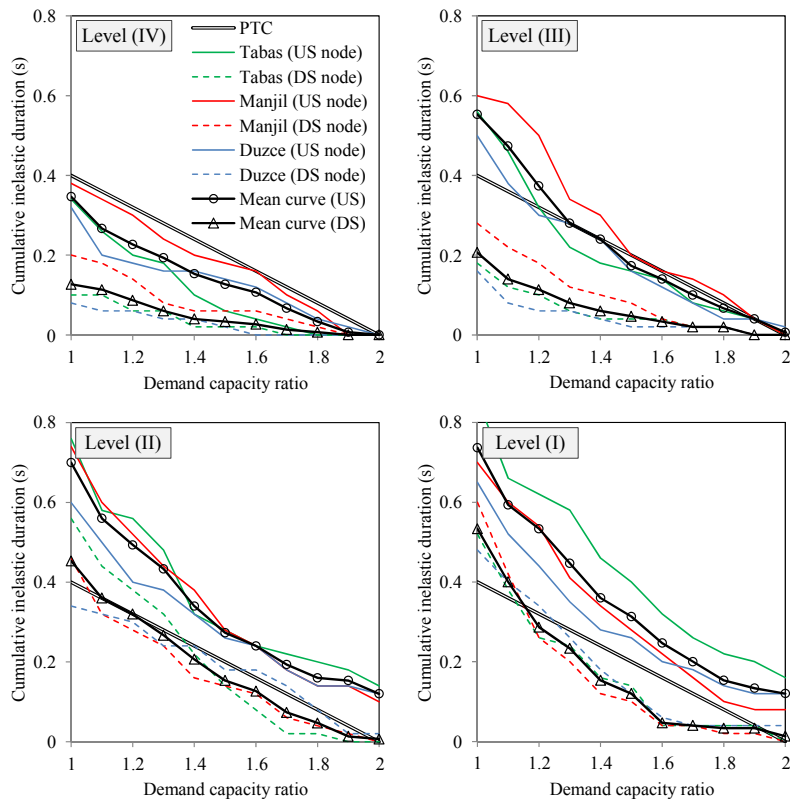


Fig. 14. Performance curves for the most representative nodes on US and DS faces of the dam body and the mean curve

## 7. CONCLUSION

In the present study, effect of the reservoir water level variation on seismic performance of a high concrete arch dam was investigated using several criteria introduced by USACE guidelines. Based on this methodology the coupled system of dam-reservoir-foundation was assumed to behave as a linear elastic system. Foundation rock and the reservoir water were assumed to be massless and compressible mediums respectively. The coupled equation of the motion for fluid-structure interaction was solved using staggered method. Four different water levels including normal water level were considered for time history analyses while the free surface sloshing was neglected due to height of the dam.

It was found that dewatering the reservoir can lead to extension of the overstressed areas on both upstream and downstream faces. The extension of the overstressed area is too intense on downstream face due to arch action of the dam body in horizontal and vertical planes. In general, increasing the reservoir water level leads to increasing of the total displacement in stream direction for the central cantilever while leading to decreasing of the first principal stresses for the upper central part of the dam. In addition, it was found that sometimes, the critical node within the dam body is not the node with the highest tensile stress. Generally, it can be concluded that operating the dam in low water levels decreases the structural safety margin for dam owners, especially in high seismicity regions. It is worthy to note that in the conducted analyses, thermal effects were not considered. However, based on the author's experience, generality of the presented conclusion is saved with or without thermal loads (due to considering seismic safety in MCE). On the other hand, it should be mentioned that the structural safety of the dam itself is different from the safety of the downstream appurtenant and the public safety. It's obvious that operating the dam in lower water levels leads to lower risk on public safety in the case of dam failure and flooding. In general, both the structural and the public safety should be considered in final decision making on safe water level for concrete dams.

## REFERENCES

1. Hariri-Ardebili, M. A., Mirzabozorg, H. & Kianoush, M. R. (2013). Seismic analysis of high arch dams considering contraction-peripheral joints coupled effects. *Central European Journal of Engineering*, Vol. 3, No. 3, pp. 549-564.
2. Fok, K. L. & Chopra, A. K. (1986). Hydrodynamic and foundation flexibility effects in earthquake response of arch dams. *ASCE: Structural Engineering*, Vol. 112, No. 8, pp. 1810-1828.
3. Fok, K. L. & Chopra, A. K. (1986). Earthquake analysis of arch dams including dam-water interaction reservoir boundary absorption and foundation flexibility. *Earthquake Engineering and Structural Dynamics*, Vol. (14), pp. 155-184.
4. Fahjan, Y. M., Borekci, O. S. & Erdik, M. (2003). Earthquake-induced hydrodynamic pressures on a 3D rigid dam-reservoir system using DRBEM and a radiation matrix. *International Journal of Numerical Methods in Engineering*, Vol. 56, pp. 1511-1532.
5. Calayir, Y., Dumanoglu, A. A. & Bayraktar, A. (1996). Earthquake analysis of gravity dam-reservoir systems using the Eulerian and Lagrangian approaches. *Computers and Structures*, Vol. 59, pp. 877-890.
6. Proulx, J., Paultre, P., Rheault, J. & Robert, Y. (2001). An experimental investigation of water level effects on dynamic behavior of a large arch dam. *Earthquake Engineering and Structural Dynamics*, Vol. 30, pp. 1147-1166.
7. Lin, G., Wang, Y. & Hu, Z. (2012). An efficient approach for frequency-domain and time-domain hydrodynamic analysis of dam-reservoir systems. *Earthquake Engineering and Structural Dynamics*, Vol. 41, pp. 1725-1749.

8. Miquel, B. & Bouaanani, N. (2013). Accounting for earthquake-induced dam-reservoir interaction using modified accelerograms. *Journal of Structural Engineering*, Vol. 139, No. 9, pp. 1608-1617.
9. Akkose, M., Bayraktar, A. & Dumanoglu, A. A. (2008). Reservoir water level effects on nonlinear dynamic response of arch dams. *Fluids and Structures*, Vol. 24, pp. 418-435.
10. Hacıfendioğlu, K., Bayraktar, A. & Bilici, Y. (2009). The effects of ice cover on stochastic response of concrete gravity dams to multi-support seismic excitation. *Cold Regions Science and Technology*, Vol. 55, No. 3, pp. 295-303.
11. Mirzabozorg, H., Akbari, M. & Hariri-Ardebili, M. A. (2012). Wave passage and incoherency effects on seismic response of high arch dams. *Earthquake Engineering and Engineering Vibration*, Vol. 11, No. 4, pp. 567-578.
12. Hariri-Ardebili, M. A. & Mirzabozorg, H. (2012). Effects of near-fault ground motions in seismic performance evaluation of a symmetry arch dam. *Soil Mechanics and Foundation Engineering*, Vol. 49, No. 5, pp. 192-199.
13. Hariri-Ardebili, M. A. & Mirzabozorg, H. (2011). Reservoir fluctuation effects on seismic response of high concrete arch dams considering material nonlinearity. *Journal of Civil Engineering Research*, Vol. 1, No. 1, pp. 9-20.
14. Ghanaat, Y. (2002). Seismic performance and damage criteria for concrete dams. *Proceedings of the 3<sup>rd</sup> US-Japan Workshop on Advanced Research on Earthquake Engineering for Dams*, San Diego, USA.
15. Ghanaat, Y. (2004). Failure modes approach to safety evaluation of dams. *Proceedings of the 13<sup>th</sup> World Conference on Earthquake Engineering*, Vancouver, Canada.
16. Yamaguchi, Y. *et al.* (2004). Seismic performance evaluation of concrete gravity dams. *Proceedings of the 13<sup>th</sup> World Conference on Earthquake Engineering*, Vancouver, Canada.
17. Bayraktar, A., *et al.* (2009). Comparison of near and far fault ground motion effects on the seismic performance evaluation of dam-reservoir-foundation systems. *Dam Engineering*, Vol. XIX, No. 4, pp. 201-239.
18. Hariri-Ardebili, M. A. & Mirzabozorg, H. (2012). Seismic performance evaluation and analysis of major arch dams considering material and joint nonlinearity effects. *ISRN Civil Engineering*, Article ID 681350, 10 pages.
19. Hariri-Ardebili, M. A. & Mirzabozorg, H. (2013). Estimation of probable damages in arch dams subjected to strong ground motions using endurance time acceleration functions. *KSCE Journal of Civil Engineering*, doi: 10.1007/s12205-013-0264-6.
20. US Army Corps of Engineers (USACE), (2007). EM 1110-2-6053: *Earthquake design and evaluation of concrete hydraulic structures*. Washington, D.C., USA.
21. US Army Corps of Engineers (USACE), (1999). EM 1110-2-6050: *Response spectra and seismic analysis for concrete hydraulic structures*. Washington, D.C., USA.
22. Ambraseys, N. N. & Douglas, J. (2000). *Reappraisal of the vertical ground motion on response*. ESEE Report00-4, Department of Civil and Environmental Engineering, Imperial College, London.
23. Campbell, K. W. & Bozorgnia, Y. (2003). UPDATED near-source ground motion (attenuation) relation for the horizontal and vertical components of peak ground acceleration and response spectra. *Bulletin of the Seismological Society of America*, Vol. 93, No. 1, pp. 314-331.
24. Boore, D. M., Joyner, W. B. & Fumal, T. E. (1997). Equations for estimating horizontal response spectra and peak acceleration from western North American earthquakes: A summary of recent work. *Seismological Research Letters*, Vol. 68, No. 1, pp. 128-153.
25. US Army Corps of Engineers (USACE), (2003). EM 1110-2-6051: *Time-history dynamic analysis of concrete hydraulic structures*. Washington, D.C.

26. Hariri-Ardebili, M. A., Mirzabozorg, H., Ghaemian, M., Akhavan, M. & Amini, R. (2011). Calibration of 3D FE model of Dez high arch dam in thermal and static conditions using instruments and site observation. *Proceeding of the 6<sup>th</sup> International Conference in Dam Engineering*, Lisbon, Portugal.
27. Hariri-Ardebili, M. A. & Mirzabozorg, H. (2013). A comparative study of the seismic stability of coupled arch dam-foundation-reservoir systems using infinite elements and viscous boundary models. *International Journal of Structural Stability and Dynamic*, Vol. 13, No. 6, DOI: 10.1142/S0219455413500326.